THE JOURNAL OF BIOLOGICAL CHEMISTRY VOL. 291, NO. 25, pp. 12930–12942, June 17, 2016

Inhibition of the Expression of the Small Heat Shock Protein αB-Crystallin Inhibits Exosome Secretion in Human Retinal Pigment Epithelial Cells in Culture*

Received for publication, October 20, 2015, and in revised form, April 14, 2016 Published, JBC Papers in Press, April 27, 2016, DOI 10.1074/jbc.M115.698530

Rajendra K. Gangalum[‡], Ankur M. Bhat[‡], Sirus A. Kohan[§], and Suraj P. Bhat[‡§¶1]

From the [‡]Jules Stein Eye Institute, Geffen School of Medicine, [¶]Molecular Biology Institute and [§]Brain Research Institute, UCLA, Los Angeles, California 90095

Exosomes carry cell type-specific molecular cargo to extracellular destinations and therefore act as lateral vectors of intercellular communication and transfer of genetic information from one cell to the other. We have shown previously that the small heat shock protein αB-crystallin (αB) is exported out of the adult human retinal pigment epithelial cells (ARPE19) packaged in exosomes. Here, we demonstrate that inhibition of the expression of αB via shRNA inhibits exosome secretion from ARPE19 cells indicating that exosomal cargo may have a role in exosome biogenesis (synthesis and/or secretion). Sucrose density gradient fractionation of the culture medium and cellular extracts suggests continued synthesis of exosomes but an inhibition of exosome secretion. In cells where αB expression was inhibited, the distribution of CD63 (LAMP3), an exosome marker, is markedly altered from the normal dispersed pattern to a stacked perinuclear presence. Interestingly, the total anti-CD63(LAMP3) immunofluorescence in the native and αB-inhibited cells remains unchanged suggesting continued exosome synthesis under conditions of impaired exosome secretion. Importantly, inhibition of the expression of αB results in a phenotype of the RPE cell that contains an increased number of vacuoles and enlarged (fused) vesicles that show increased presence of CD63(LAMP3) and LAMP1 indicating enhancement of the endolysosomal compartment. This is further corroborated by increased Rab7 labeling of this compartment (Rab-GTPase 7 is known to be associated with late endosome maturation). These data collectively point to a regulatory role for αB in exosome biogenesis possibly via its involvement at a branch point in the endocytic pathway that facilitates secretion of exosomes.

Exosomes are 50–200-nm nanovesicles produced via the endosomal pathway of protein homeostasis (1–3). The process of endocytosis and the trafficking of endocytosed vesicles to lysosomes are major pathways of protein metabolism that regulate transmembrane protein (receptor) turnover at the plasma membrane. The exosome biogenesis starts with the early endosome that matures into a late endosome concomitant with its intraluminal vesicles, making it a multivesicular body (MVB).[2] The MVB is at a branch point of this pathway from where it may progress toward two different cellular compartments with two entirely different physiological consequences. The first one is that the MVB may fuse with the lysosomes (generating the endolysosomal compartment) leading to the degradation of its vesicular contents; the second is that the MVB traffics to and fuses with the plasma membrane, leading to the release of its intraluminal vesicles as exosomes carrying the active macromolecular cargo. What dictates either of the two fates is not known (4).

RPE is an important single layer of cells at the interface of the blood-retina barrier. It provides critical physiological support for the maintenance of the photoreceptor neurons (5, 6). It is a polarized epithelium, which on its apical side nourishes the neuronal compartment within the eye and on its basal side interacts with the systemic input. These cells constitutively express αB-crystallin (αB), an archetypical member of the small heat shock family of proteins whose expression has been associated with age-related macular degeneration (7), a dysfunction of the aged RPE that leads to the loss of retinal photoreceptors and eventual blindness. Importantly, the expression of this small heat shock protein also attends many neurodegenerations, including Alzheimer disease, Parkinson disease, multiple sclerosis, and a wide range of pathologies, including breast cancer and cardiomyopathies (8–10).

αB is a 20-kDa membrane-associated small heat shock protein (11–15) that is known to possess anti-aggregation properties *in vitro* (10). In addition to being a crystallin (a protein expressed at relatively high levels in the ocular lens), it is expressed in many tissues in a developmentally dictated fashion (16). It is expressed very early during cardiac development and in the normal developing brain where it is seen predominantly in oligodendrocytes and astrocytes (17); it has been identified as the chief antigen in multiple sclerosis (18).

Although it is expressed in a large number of tissues, this small heat shock protein is not found in all cell types. It is expressed constitutively in many epithelial cells, including the ARPE19 cell line (derived from the adult human retinal pig-

* This work was supported by NEI, National Institutes of Health grant 1R01EY024929 (to S. P. B.) and the Gerald Oppenheimer Family Foundation for the Prevention of Eye Disease Endowment Fund. The authors declare that they have no conflicts of interest with the contents of this article. The content is solely the responsibility of the authors and does not necessarily represent the official views of the National Institutes of Health.

[1] To whom correspondence should be addressed: 100 Stein Plaza, Geffen School of Medicine, UCLA, Los Angeles, CA 90095. Tel.: 310-825-9543; E-mail: bhat@jsei.ucla.edu.

[2] The abbreviations used are: MVB, multivesicular body; αB, αB-crystallin; TEM, transmission electron microscopy; PFA, paraformaldehyde; AChE, acetylcholine esterase; RPE, retinal pigment epithelium; ARPE, adult human retinal pigment epithelial cell line.

ment epithelium) but not in many fibroblasts (19). In fibroblasts, this protein is expressed in response to physical stress such as exposure to higher temperatures (20). Significantly, when introduced into cells it provides protection against heat shock and makes cells resistant to apoptosis (9, 21).

αB is not a secretory protein; however, its export, packaged in exosomes (22), can have vital physiological consequences when taken up by cells that do not express this protein. Therefore, we ask the following question. Do cells that package proteins, like αB for extracellular distribution, involve these proteins (which constitute the exosomal cargo) in any regulatory function that modulates the biogenesis (synthesis and/or secretion) of the exosome?

Exosomes carry gene products that are representative of the developmental and/or the physiological state of a cell, and therefore, the production of the exosomes and what is packaged in them may be interactively connected and regulated (23, 24). However, beyond the elucidation of the canonical activities (25–29) that would be required for exosome assembly in any cell, it is unknown at this time whether there is a role, if any, for the exosomal cargo (proteins that are intended for extracellular destinations) in the exosome biogenesis.

In view of the cell type specificity of the αB expression (19, 20) and its secretion via exosomes, the ARPE19 cell line presents an amenable paradigm for investigating the regulation of the biogenesis of the exosomes by exosomal cargo. As a representative of the exosomal cargo that is sent outside of the RPE, we sought to examine the impact of the inhibition of the expression of αB on exosome biogenesis as assessed by sucrose density gradient analyses, immuno-confocal microscopy, double immunogold labeling, and transmission electron microscopy (TEM).

We inhibited the constitutive expression of αB in the ARPE19 cells employing specific shRNAs. Multiple clones transfected with different shRNAs showed loss of αB expression. Transfected αB shRNA clones that did not show inhibition of αB expression and/or cells transfected with scrambled αB sequences (which also did not show inhibition of αB expression) and the native ARPE19 cultures were used as the control cells. We provide evidence that the exosomal cargo (represented here by αB) has an important role in exosome biogenesis.

Experimental Procedures

Cell Culture and Isolation of Exosomes—ARPE19 cells (ATCC, Manassas, VA) were maintained at 70% confluence in Dulbecco's modified Eagle's medium with nutrient mixture Ham's F-12 (DMEM/Ham's F-12, 1:1 ratio) containing 10% exosome-depleted fetal bovine serum (FBS) and antibiotics, in a humidified incubator (95% air, 5% CO_2) at 37 °C.

For isolation of exosomes, the cells were washed three times with 1× phosphate-buffered saline (PBS without Ca^{2+} and Mg^{2+}, pH 7.4) followed by two washes with serum-free DMEM/Ham's F-12 (1:1) and allowed to grow in the same serum-free medium. This medium was collected 12–14 h later for isolation of exosomes.

Stable Transfection and Inhibition of αB Expression—Four αB shRNA HuSH-29 plasmid constructs containing the sequences shown below, one scrambled shRNA sequence, and the empty vector were purchased from OriGene Technologies, Inc. Rockville, MD: 1) TGGTTTGACACTGGACTCTCAGAGATGCG; 2) TCTCTGTCAACCTGGATGTGAAGCACTTC; 3) TGTGACTAGTGCTGAAGCTTATTAATGCT; 4) GTCCTCACTGTGAATGGACCAAGGAAACA; 5) GCACTACCAGAGCTAACTCAGATAGTACT (ineffective scrambled sequence, control), and 6) pGFP-V-RS, the empty vector.

ARPE19 cells were transfected with 1 μg of the recombinant plasmid using Neon Transfection System (Invitrogen) employing two pulses (1350 V for 20 ms each). Cells were allowed to grow for 2 days and then selected against 100 ng/ml puromycin (Invitrogen) for 2 weeks, replenishing the medium every 2 days. Individual clones were isolated using cloning cylinders (Sigma). The stable cell lines were maintained in puromycin; passages 4–6 of these clones were used in all experiments. The cells were morphologically examined using the FSX100 Olympus microscope, after staining with trypan blue (Fig. 1*E*).

Discontinuous Sucrose Density Gradient Fractionation—Cells were lysed in homogenization buffer (0.5 M sucrose, 10 mM potassium phosphate, and 5 mM $MgCl_2$, pH 6.7) containing protease inhibitor mixture (ThermoFisher Scientific). The post-nuclear supernatants were fractionated on 2.2-ml discontinuous sucrose gradients as described (22), and the presence of vesicles was assayed by AChE activity (30). Twenty fractions (~100 μl each) were collected and concentrated to 50 μl using 3000 MWCO Millipore concentrators. 5 μl from each fraction were used for SDS-PAGE and immunoblotting (22). The same procedure was followed for analysis of the culture medium after concentration. As a control, in these experiments note that the AChE activity and αB and HSP70, profiles are resistant to 0.1 and 1.0% Triton X-100 (Fig. 4*C*).

Antibodies—Primary antibodies used in this study were: anti-rabbit polyclonals, anti-αB crystallin (13) (Sigma Genosys); anti-Flotillin-1, anti-HSP70, and anti-Alix, (Santa Cruz Biotechnology); anti-Rab7, anti-Rab5, and anti-Enolase1 (Cell Signaling Technologies). Anti-HSP60 (Abcam) and anti-HSP90β (StressGen) are mouse monoclonal antibodies. Appropriate horseradish peroxidase (HRP)-linked secondary antibodies were used to detect proteins on immunoblots, using the West Dura SuperSignal Extended Duration Substrate (Pierce). The total cell extract (35 μg) from native ARPE cells was used as a reference for immunoblotting (22). In Fig. 3 the following polyclonal antibodies were used: anti-THBS1 (thrombospondin 1), anti-C3 (complement component 3), anti-QSOX1 (quiescin Q6 sulfhydryl oxidase 1), anti-PAI (serpin peptidase inhibitor, Clade E (Nexin, Plasminogen Activator Inhibitor Type 1), anti-ANXA2 (Annexin II), Member 1), (GeneTex, Irvine, CA). Anti-CYC (Cytochrome *c*) was purchased from Abcam.

Quantitation of Exosome Secretion Using NRhPE Dye Assay—ARPE cells were seeded (2×10^5 per well) in transwell permeable inserts (6 well, 0.4 μm polyester membrane, 24 mm insert) (Corning Life Sciences, Pittston, PA). The medium was replenished every 2 days and cells were allowed to form monolayers for 30 days. The trans-epithelial resistance (TER) was measured weekly (at 30 days it was 186 ± 12 Ωcm^2). Exosomes were isolated from the culture medium as described previously (22).

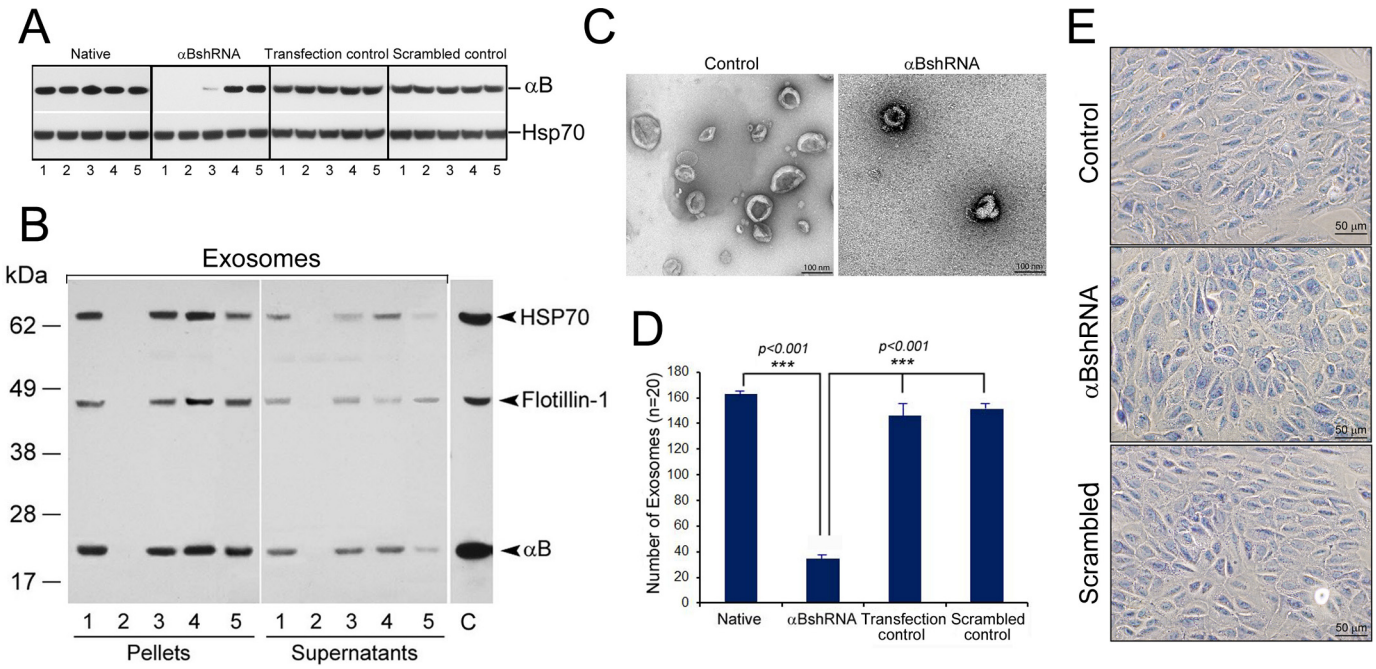

FIGURE 1. **Inhibition of the expression of αB inhibits exosome secretion.** *A,* immunoblot for assessing αB expression in ARPE clones transfected with αB shRNA plasmids (total cell extracts, 30 μg/lane). *Native* = five different cultures, *lanes 1–5*; *αB shRNA* = five independent clones, *lanes 1–5*; *Transfection control* = cells transfected with different shRNA constructs that do not inhibit αB expression, five clones, *lanes 1–5*; *Scrambled control* = cells transfected with a scrambled shRNA sequence that is not expected to inhibit αB expression, five clones, *lanes 1–5*. Empty vector construct and other shRNA constructs that did not inhibit expression are not shown. Only the relevant areas of the immunoblots are shown, the one showing reaction against αB antiserum and the other against HSP70 antiserum. HSP70 acts as a loading control. *B,* immunoblot of the exosomal pellets and the supernatants prepared from the culture media of various shRNA clones identified in the screen shown in *A* (*lane 2* from each immunoblot). *Lane 1,* exosomal pellet from native ARPE cells; *lane 2,* an ARPE clone permanently transfected with an shRNA construct where the expression of αB is inhibited (*lane 2* in Fig. 1*A*, *αB shRNA panel*); *lanes 3* and *4* are constructs that do not impact αB expression (represented by the *Transfection control* panel clones shown in Fig. 1*A*); *lane 5* is one of the clones from the panel *Scrambled control* shown in Fig. 1*A*. No exosome markers are detected in *lane 2* (*clone #2*). *Lane C,* control, a cell extract from native transfected ARPE cells, different from *lane 1*, which contains proteins from the exosomal pellet isolated from native ARPE cells. *C,* electron micrographs of negatively stained exosomal pellets made from *Control* (cells transfected with a scrambled sequence) and from clone #2 where αB expression is silenced (*A*, *αBshRNA, lane 2*). *D,* quantitation of the number of exosomes in the electron micrographs ($n = 20$) shown in *C*. *E,* micrographs of the *Control* (Native ARPE), αB shRNA (ARPE transfected with clone #2, which does not express αB) and Scrambled (ARPE cells transfected with a scrambled sequence).

NRhPE phospholipid fluorescent analog (N-lissamine rhodamine B sulfonyl phosphatidylethanolamine) was prepared according to manufacturer's instructions (Avanti Polar Lipids, Alabaster, AL) (32). The ethanol soluble fluorescent phospholipid was added to serum-free DMEM/Ham's F-12 (0.5% v/v) with vigorous vortexing and added to cell cultures. After incubation for 30 min at 4 °C, the culture medium was removed and the cells were washed with ice cold PBS to remove excess unbound dye. Labeled cells were then incubated in complete RPMI medium at 37 °C for six h. after which the medium was collected for exosome isolation. The exosome pellet was dissolved in 30 μl of PBS. 15 μl of this was diluted with 1.0 ml PBS containing 0.1% Triton X-100. The released dye was measured using Fluorescence Spectrophotometer (Varian, Cary Eclipse, Walnut Creek, CA) (excitation, 560 nm and emission, 590 nm). The error bars in Fig. 2 represent mean absorbance values ($n = 3$) ± S.E.

Live Cell Staining with Lysotracker—Lysotracker Red DND-99 (20 nM, Molecular Probes, Invitrogen) was incubated with cells for 2 min in serum-free DMEM/F12 (1:1) medium at room temperature. After incubation, cells were washed thoroughly with PBS (1X), fixed briefly in 2% paraformaldehyde (PFA) and mounted and observed (FluoView 1000 Olympus Confocal Microscope) with excitation filters 510–560 nm and barrier filter 590 nm. The images were acquired and annotated using Adobe Photoshop Elements, version 9.0.

Immunofluorescence and Confocal Microscopy—Cells were fixed in ice cold methanol for 6 min at −20 °C and washed with PBS (1×). Fixed cells were blocked in PBS containing 5% goat serum, 1.0% BSA, 0.2% Triton X-100 (1×) for 45 min and then double labeled sequentially with Anti-αB and anti-CD63 (LAMP3). The primary antibodies were used at 1:250 dilutions, TRITC or FITC labeled secondary antibodies were used at 1:300 dilutions. The images were acquired with FluoView 1000 Olympus confocal microscope (Objective lens = PLANON O SC ×60, NA = 1.40, Pinhole = 1 Airy unit, Z dimension = 0.5 μm/slice) as before (22).

Electron Microscopy and Immunogold Labeling—The cells were washed three times with 1× PBS to remove the serum containing medium and fixed in 2% Glutaraldehyde (Glut) and 2% PFA in 0.1× PBS, pH 7.4, for 2 h. at room temperature. Cells were gently scrapped, collected in round bottom tubes and further incubated overnight in the fixative mix at 4 °C. Next day, 0.5% of tannic acid was added to the cells and incubation continued for one more h at room temperature. The cells were then washed five times in 0.1× PBS buffer and post-fixed in a solution of 1% OsO_4 in PBS, pH 7.4. The combination of Tannic acid/Glut/PFA followed by osmification increases the staining

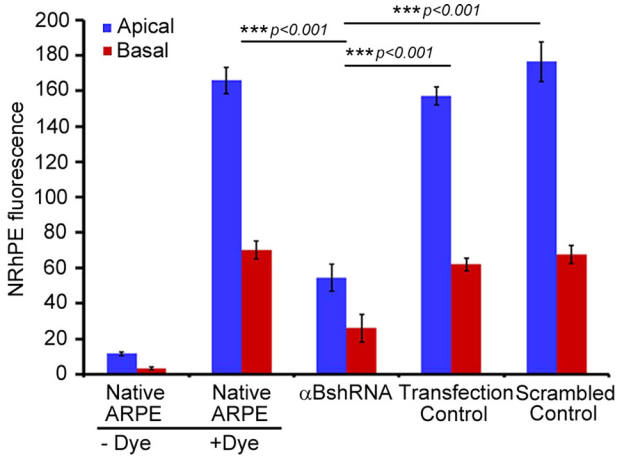

FIGURE 2. **Inhibition of exosome secretion from apical and basal surfaces in αB silenced ARPE cells.** Confluent monolayers of ARPE19 cells grown on transwell inserts were used to study the apical and basal exosome production using the NRhPE dye, a fluorescent lipid that is internalized by endocytosis and labels exosomes/MVBs (32). The cells were incubated with the NRhPE dye in serum-free medium, washed, and then incubated in the dye-free medium. Exosome preparations obtained from apical and basal medium were used to measure the total fluorescence as an indicator of exosome secretion into the medium (see under "Experimental Procedures"). The ARPE cells (*αBshRNA*), where αB expression is inhibited, show appreciable decrease in total fluorescence from both apical as well as basal surfaces indicating inhibition of exosome secretion from the apical as well as basal surfaces. *αBshRNA* = ARPE cell clone where αB expression was inhibited (Fig. 1*A*, *αB shRNA, lane 2*); *Transfection control* = αB shRNA transfected ARPE where there was no inhibition of the expression of αB (Fig. 1*A*, *Transfection control*); *Scrambled control* = ARPE cells transfected with a scrambled αB shRNA sequence that does not inhibit αB expression (Fig. 1*A*, *scrambled control*).

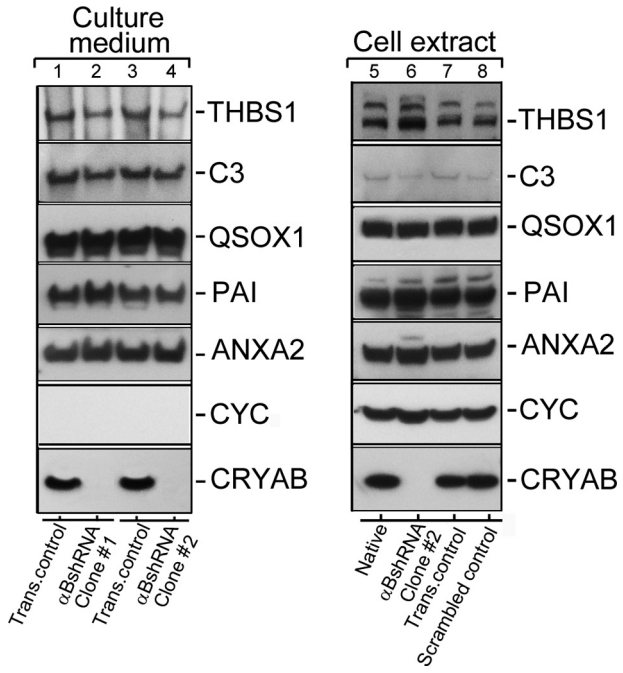

FIGURE 3. **Conventional protein secretion in αB-silenced ARPE cells.** Immunoblots of known extracellular proteins of the ARPE19 cells (in the culture medium and cellular extracts) are shown. 40 μg of protein were run on each lane on an SDS-polyacrylamide gel (gradient 4–12%; Life Technologies, Inc.), transferred to a membrane, and probed with following polyclonal antibodies (*left panel* shows the *Culture medium,* and the *right panel* shows total *Cell extract* immunoblots, respectively): anti-THBS1 (thrombospondin 1); anti-C3 (complement component 3); anti-QSOX1 (quiescin Q6 sulfhydryl oxidase 1); anti-PAI (serpin peptidase inhibitor, clade E (nexin, plasminogen activator inhibitor type 1), member 1); anti-ANXA2 (annexin II); anti-CYC (cytochrome *c*); and anti-αB (αB-crystallin, CRYAB). Two different clones of ARPE19 cells, permanently transfected with αB shRNA plasmids, that do express αB (*lanes 2* and *4*) were analyzed (*Culture medium; left panel*). All five proteins that were expected to be in the medium (as per conventional protein secretion) were detected in transfection control (*Trans. control*, *lanes 1* and *3*). *Lanes 2* and *4* show absence of αB in the medium of ARPE αB shRNA clones #1 and #2 respectively. Note that cytochrome *c* (*CYC*) is not detected in the culture medium of all four cultures indicating that there is no cell death. The *right panel* shows immunoblots of the cell extracts from the *Native* un-transfected cells (*lane 5*), *αBshRNA clone #2* (*lane 6*, αB-crystallin is silenced), transfection control (*lane 7*), and *Scrambled* shRNA control (*lane 8*), where αB-crystallin is not silenced. Based on these data, conventional protein secretion is not directly impacted by the absence of αB expression. In this immunoblot only αB shRNA clone #2 was used (*lane 6*).

of the membranes. The samples were washed four times in sodium acetate buffer, pH 5.5, block-stained in 0.5% uranyl acetate in 0.1 M sodium acetate buffer, pH 5.5, for 12 h at 4 °C, dehydrated in graded ethanol (50, 75, 95, 100, 100, 100%; 10 min each), passed through propylene oxide, and infiltrated with mixtures of Epon 812 and propylene oxide (1:1 first and then 2:1) for two h each. The cells were then infiltrated with pure Epon 812 overnight. Embedding was performed in pure Epon 812 and curing was done at 60 °C for 48 h. Sections of 60 nm thickness (gray interference color) were cut on an Ultramicrotome (MT-X, RMC, Tucson, AZ) using a diamond knife. The sections were deposited on single-hole grids coated with Formvar and carbon; double-stained in aqueous solutions of 8% uranyl acetate for 25 min at 60 °C and lead citrate for 3 min at room temperature and finally examined with a 100CX JOEL electron microscope.

For the immunogold labeling the cells were fixed in 4% PFA and 0.1% Glut for 2 h. at room temperature. Cells were embedded in LR white resin employing a slightly modified published procedure (33). Ultra-thin (60 nm) sections of cells were collected on nickel grids and pre-incubated for 20 min with a drop of Tris-buffered saline containing 50 mM glycine and 0.001% $NaBH_4$. The grids were rinsed and blocked with 1:20 dilution of normal goat serum (Pierce) in Tris-buffered saline and then incubated with two different antibodies in one of the following combinations sequentially: 1) Anti-CD63(LAMP3) and anti-LAMP1, 2) Anti-Rab5 and anti-Rab7, each at 1:100 dilutions. The grids were washed with Tris-buffered saline thoroughly and incubated with appropriate secondary antibody tagged to either 12-nm or 18-nm gold particles (1:200 dilution) following a standard protocol (34).

For TEM of the exosomes, the exosome pellets were examined by negative staining as detailed previously (33).

Image Processing and Statistical Analysis—Immuno-fluorescence in confocal images (CD63(LAMP3) and Lysotracker) was quantified using ImageJ analysis software (National Institute of Health, Bethesda, MD. Java 1.6.0_20 (64-bit), Version 1.48v). For CD63 Tiff images (300 dpi, RGB or gray scale) were analyzed with free hand tools to select the whole cell and/or particle (n = 110).

Lysotracker images (300 dpi, RGB or gray scale, n = 50), were analyzed with free hand line tool to obtain plot profiles (Fig. 6*C*). For generating three-dimensional surface plots (Fig. 5*B* and 6*B*), the ImageJ three-dimensional viewer plugin (.jar file) was loaded. Plugin tab was used to open interactive three-dimensional surface plot in three dimensions. The confocal image of ARPE cells stained with CD63-FITC shown in inter-

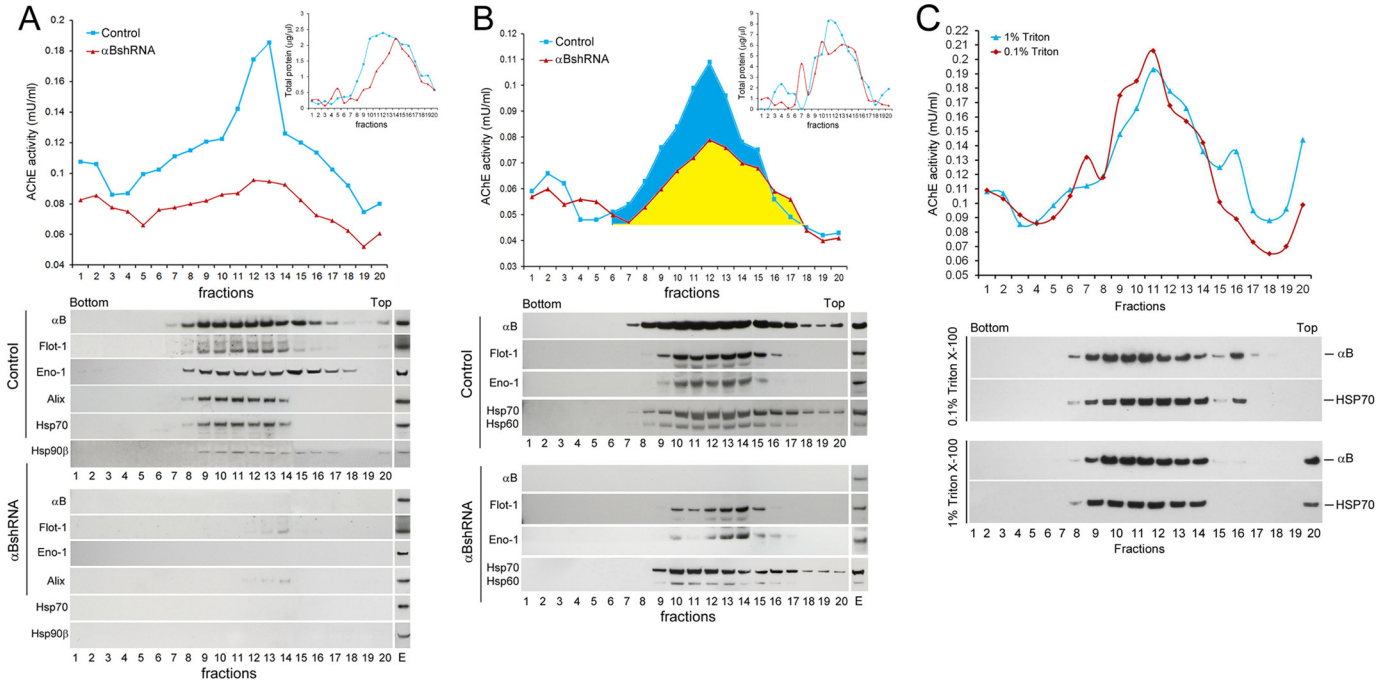

FIGURE 4. **Status of the synthesis of vesicles in αB-silenced ARPE cells.** *A,* profile of AChE activity (*top panel*) and exosomal markers (*bottom panels*) in discontinuous sucrose density gradient of the culture medium from control (*blue*) and αB-silenced (*red*) ARPE cells. The AChE activity is appreciably reduced (*red*) and the exosomal markers αB, Flotillin 1 (*Flot-1*), Enolase 1 (*Eno-1*), Alix, Hsp70, and Hsp90β, as analyzed by immunoblotting are barely detectable (*bottom panels*), consistent with the absence of exosomes in the medium from αB-silenced cells (*αBshRNA*). *B,* discontinuous sucrose density gradient fractionation of cellular extracts. There is about 50% loss of AChE activity (compare *blue* and *yellow area*). Note the presence of exosomal markers (*Flot-1, Eno-1, Hsp60*, and *Hsp70*; anti-Alix and anti-Hsp90β were not used here) (*bottom panels*) in the fractions containing the AChE activity, suggesting continued synthesis of exosomes. *E* = native ARPE cellular extract (30 μg). *Fractions 1* and *20* represent the bottom and the top of the gradient, respectively. Total protein profiles are presented as *insets* in the respective *top panels*. It is important to note that these cells were cultured in serum-free medium. *C,* this is a control gradient run with Triton X-100-treated medium from the native ARPE cells. *Top panel* shows profile of the AChE activity and the *bottom two panels* show immunoblots of fractions collected from each gradient. The samples were treated with Triton X-100 for 30 min at 4 °C (*red,* 0.1%, and *blue,* 1% Triton X-100) before loading on the gradient. Triton X-100 does not alter the AChE activity nor the immunoblot profiles markedly.

active three-dimensional surface plot is generated at the following settings (Mesh; Fire LUT; with optional Display Options: Grid Size, 256; Smoothing, 7.5; Perspective, 0.17; Lighting, 0.2; check the z-Ratio xy-Ratio; Scale, 1.81; Z-scale, 0.87; Max, 28%; Min, 0%) for control, scrambled and αB shRNA (Fig. 5*B*). For the LysoTracker staining the interactive three-dimensional surface plot parameters were adjusted (Mesh; Fire LUT; with optional Display Options: Grid Size, 512; Smoothing, Perspective and Lighting to zero; check the z-Ratio xy-Ratio; Scale, 1.02; Z-scale, 0.33; Max, 33%; Min, 0%) to generate the images shown in Fig. 6*B*.

For the immunoblotting data, the reaction bands on x-ray films were scanned in white light and quantified using FluorChem Q, MultiImage III (Alpha Innotech Corporation).

The number of gold particles in electron micrographs of CD63(LAMP3)/LAMP1 and Rab5/Rab7 ($n = 20$ from each group) were quantified by using ImageJ, particle analysis. Statistical analysis was performed with Microsoft Excel. Statistical significance was evaluated with the student *t* test, according to the following description: not significant (NS); and $p < 0.001$, highly significant (***). All values from quantitative data are reported as mean ± S.E. from 'n' independent groups of cells. Error bars in Figs. 1, 2, 5, 6, 8 and 9 represent the S.E.

Results

Inhibition of αB Expression Inhibits Exosome Secretion—We transfected ARPE19 cells with various shRNA plasmid constructs to silence αB expression and generated multiple independent clones for each construct (which included four constructs for αB mRNA, one with scrambled sequence and one with an empty vector). Out of the four αB constructs, we picked five independent clones from the one αB shRNA construct that looked promising (Fig. 1*A*, *αB shRNA*). We also picked five clones (represented by *lanes 1–5* each in Fig. 1*A*) for all other constructs. Note that in Fig. 1*A*, αB shRNA, clones 1, 2 and 3 (*lanes 1–3*) show significant inhibition of αB expression. We picked clone # 1 and clone # 2 for initial analysis and then concentrated on clone # 2 for further analysis. We also picked clones represented by *lane 2* in all the immunoblots (Fig. 1*A*), cultured them, isolated the exosome pellets from their media and immunoblotted them for exosome markers (HSP70, Flotillin-1 and αB) (22). These exosomal markers are seen in all lanes except in *lane 2* (Fig. 1*B*), which represents the medium from the cell line clone #2, which does not make any detectable αB (Fig. 1*A*, *αB shRNA, lane 2*) indicating that the culture medium of this cell line contains very few exosomes. This conclusion is corroborated by TEM of the exosome pellets (Fig. 1, *C* and *D*). None of these ARPE clones show any signs of apoptosis (Fig. 1*E*) although the clones with inhibited αB expression showed slower growth.

RPE is a polar epithelium. It secretes exosomes from both the basal as well as apical sides (22). The native ARPE19 cells and cells stably transfected with αB shRNA #2 (Fig. 1*A*, *αB shRNA, lane 2*) were grown on transwell inserts (22) and assessed for the

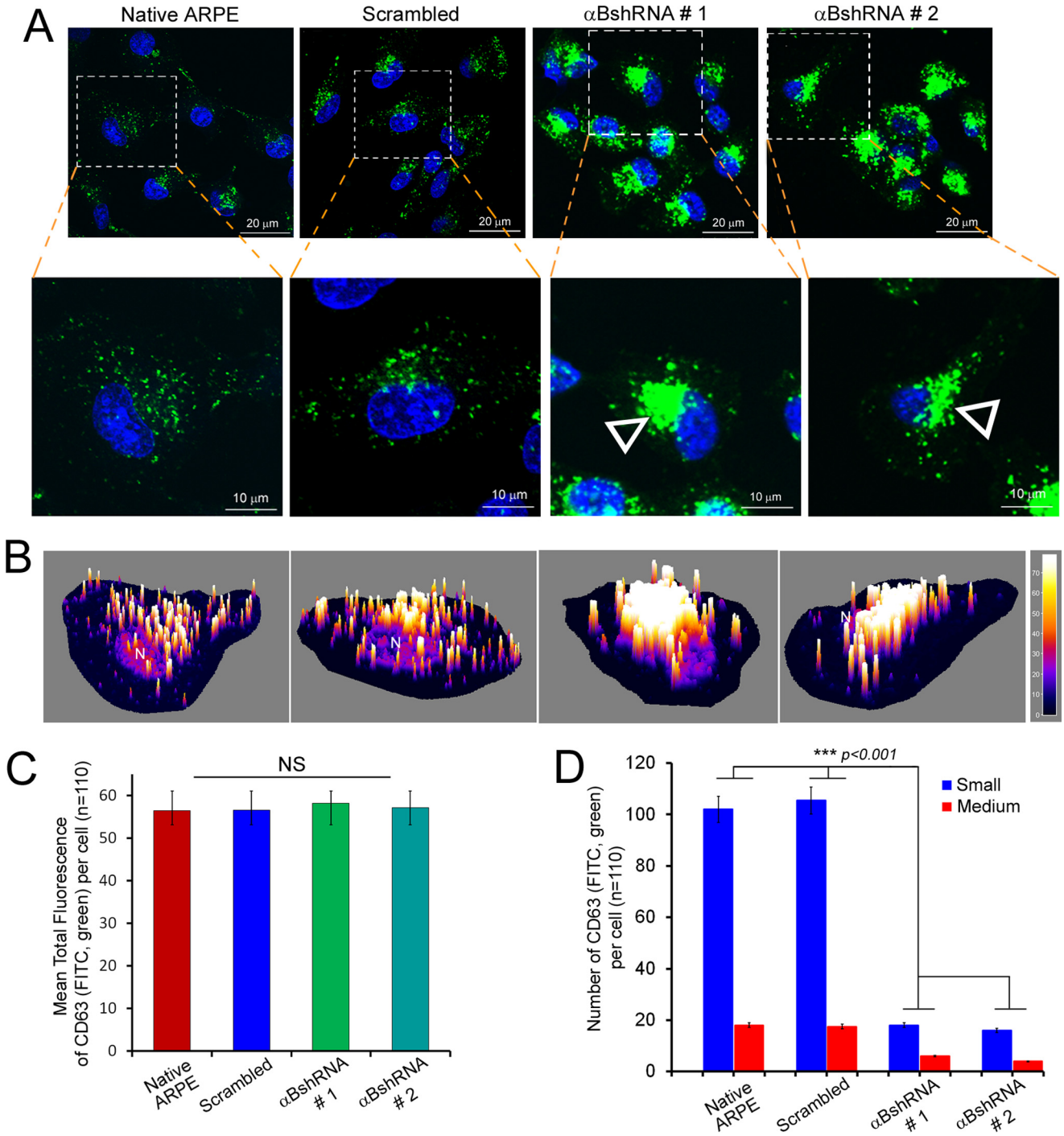

FIGURE 5. **Inhibition of αB expression leads to aggregated patterns of CD63 (LAMP3) distribution.** *A,* confocal images of ARPE cells (*z*-sections) showing distribution of CD63(LAMP3) (FITC, *green*)-labeled vesicles. A magnified view of the corresponding individual *z*-slice (0.5 μm) from a single cell is shown on the *bottom panel*. Note that in native and scrambled control cells the CD63(LAMP3)-labeled vesicles are dispersed throughout the cytoplasm, while there is a peri-nuclear accumulation of these vesicles (*open arrowheads*) in αB-silenced cells (*αB shRNA #1* and *αB shRNA #2*). *B,* three-dimensional surface plots of the *z*-slices magnified in *A*. *C,* quantitation of CD63(LAMP3) cellular fluorescence in the *z*-slices shown in *A*. Although the perinuclear accumulation of CD63(LAMP3) fluorescence in αB-inhibited cells (*αB shRNA #1* and *αB shRNA #2*) appears increased, there is no significant difference in the total anti-CD63 fluorescence in all four groups of cells. *D,* quantitation of the number of vesicles. There is significant difference in the distribution of vesicles in the αB shRNA cells where the vesicles are largely stacked and are therefore not counted as single units as in the native ARPE and in scrambled control cells. Note that the vesicles were grouped as *Small* (≤120 nm) and *Medium* (≥121 nm); note that the data clearly indicate large changes in both categories because of the stacking and/or fusion in αB-silenced cells.

secretion of exosomes by the NRhPE dye assay (32). The data in Fig. 2 establishes that the inhibition of αB expression inhibits exosome secretion, from the apical as well as the basal surfaces of the ARPE19 cells (Fig. 2, *αB shRNA*).

Conventional Protein Secretion in αB-inhibited ARPE Cells—It is unclear if there is a distinction between the exosome-related secretion and the signal peptide-dependent conventional secretion. We assessed the status of five different proteins pre-

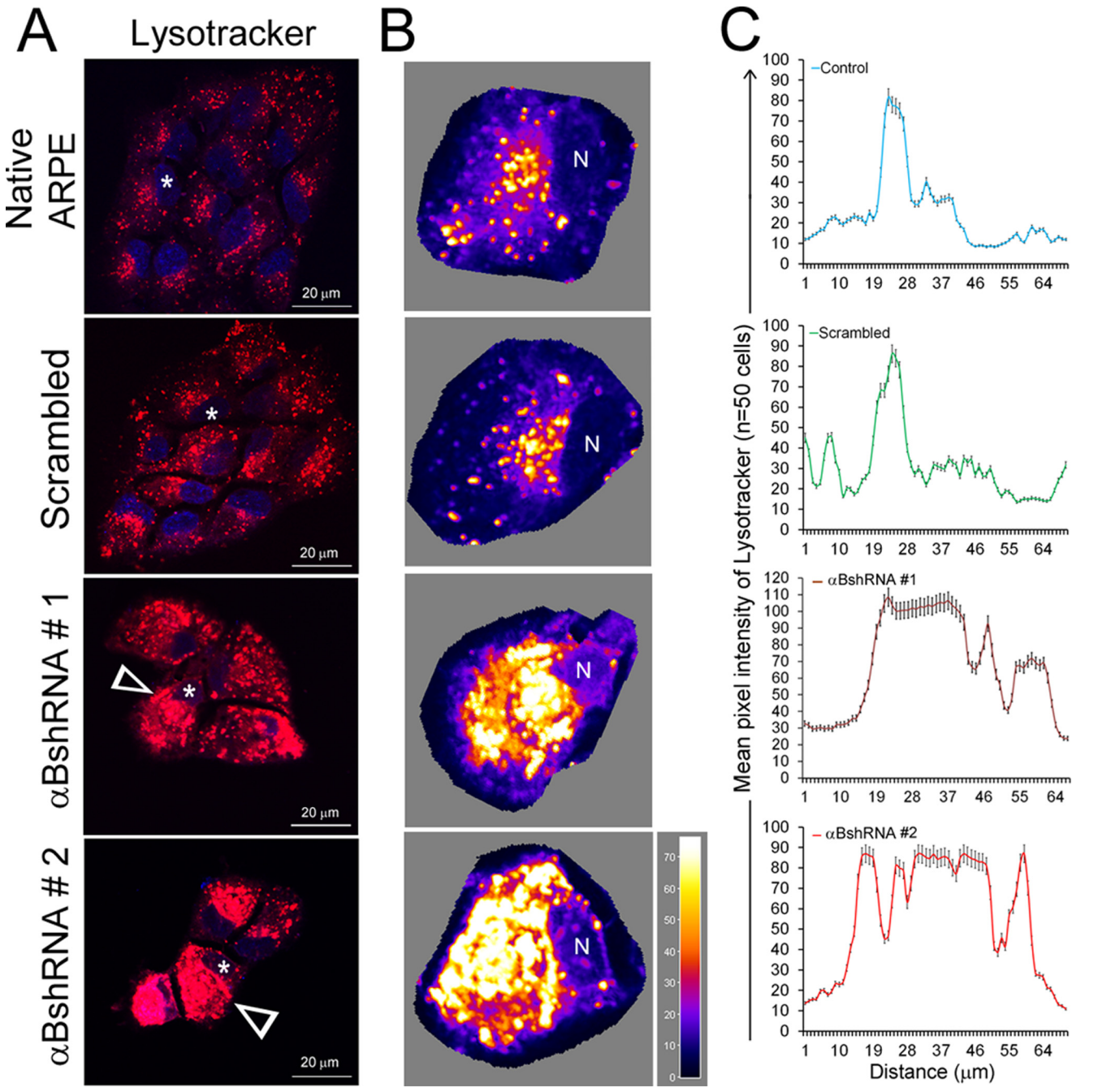

FIGURE 6. **Inhibition of αB expression leads to altered patterns of lysosomal staining in αB-inhibited ARPE cells.** *A,* live cell images of ARPE cells incubated in Lysotracker Red DND-99 (that stains the acidic organelles in *red*) show a dispersed pattern in native and scrambled control ARPE cells (*upper two panels*). However, in cells where αB expression is inhibited, clumped or aggregated staining is seen (*αB shRNA #1* and *αB shRNA #2*, *white arrowheads*). *B,* three-dimensional surface plots of individual cells shown by *asterisks* in *A*. The images were oriented such that the cellular nucleus (*N*) was on the same side. The pseudocolor scale shows intensity. *White,* high; *dark blue,* low. *C,* quantitation of distribution of LysoTracker fluorescence in native (*blue line*), scrambled (*green line*), and *αBshRNAs #1* and *#2* (*brown* and *red lines*, respectively) ARPE cells using ImageJ plot profiles (mean pixel intensity is expressed ± S.E.). αB-silenced ARPE cells show multiple high mean peak pixel intensities across the cytoplasm indicating altered distribution of lysosomal components.

viously known to be present in the culture medium of ARPE19 cells (35). The native and the αB shRNA-inhibited cells were grown, and their media were concentrated and examined for the presence of proteins that may not be related to exosomal secretion pathway. Five proteins THBS1 (thrombospondin 1), C3 (complement component 3), QSOX1 (quiescin Q6 sulfhydryl oxidase 1), PAI (serpin peptidase inhibitor, clade E (nexin, plasminogen activator inhibitor type 1, member 1), and ANXA2 (annexin II) were arbitrarily selected from the published data (35). Fig. 3 shows immunoblots from the culture media and the cell extracts. There is very little difference in the presence of all these proteins in the extracellular media of native and scrambled αB shRNA ARPE cells and in ARPE cells where αB expression is inhibited (Fig. 3, *culture media, lanes 2* and *4*, which represent media from two independent ARPE αB shRNA clones #1 and #2, respectively). This suggests that αB inhibition in ARPE19 cells largely impacts the exosome-related secretion. Based on the data obtained thus far on ARPE clones

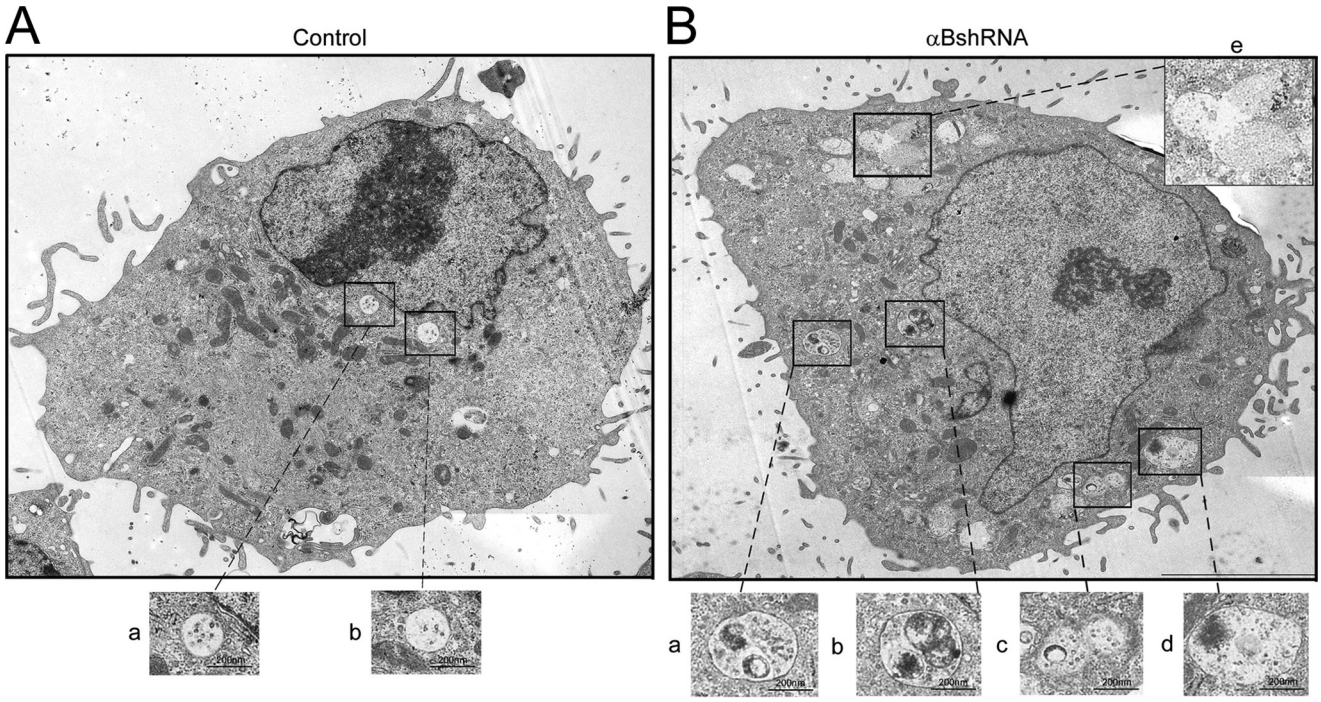

FIGURE 7. **αB-silenced ARPE cells show enhanced vesicles and vacuolar fusion.** *A,* electron micrograph of a control ARPE cell (scrambled shRNA control) showing endosomes and MVBs (magnified images *panels a* and *b, bottom*) in the perinuclear region with various other cell organelles (mitochondria, endoplasmic reticulum, and Golgi complex) (*B*), electron micrograph of an αB-silenced ARPE cell (*αBshRNA*). Note the presence of a large number of vacuoles all over the cytoplasm. There are abnormal vesicles, which may represent fused endosomes/MVBs and endo-lysosomes (see *boxed* and *magnified images* in *panels a–e*). Note that there is a lot of electron dense material in most of the fused vesicles. *Scale bars,* 200 nm.

(αB shRNA #1 and #2) (Figs. 3–5), we focused on clone #2 for the rest of this investigation.

Sucrose Density Gradient Profiles of the Culture Medium and Cellular Extracts—To gain insight into the synthesis of exosomes, we fractionated the culture media and cellular extracts of control and αB-silenced cells on discontinuous sucrose density gradients (Fig. 4). The presence of vesicles was ascertained by assaying for AChE activity in each gradient fraction (30). Fractionation of the culture medium shows a large reduction in the AChE activity (Fig. 4*A*) and an almost complete absence of exosomal markers (flotillin1, alix, enolase 1, Hsp70, and Hsp90*β*) in the medium from αB-silenced ARPE cells (Fig. 4*A*, *bottom panels*). These data are consistent with the significant reduction of exosomes in the culture medium of cells where αB expression is inhibited (Fig. 1, *B–D*).

Fractionation of cell extracts, however, shows only about 50% reduction in the AChE activity, suggesting that vesicular synthesis is not completely halted (Fig. 4*B*, *redline, yellow area*). This is corroborated by the presence of exosome markers (flotillin1, enolase 1, Hsp70, and Hsp60) in the fractions that contain the AChE activity (Fig. 4*B*, *bottom panels*). These data suggest continued synthesis of exosomes under conditions of impaired secretion in αB-silenced cells.

Inhibition of αB Expression Results in Aggregated Staining Patterns of CD63(LAMP3)—ARPE19 cells, stably transfected with αB shRNA that inhibits the αB expression, were immunostained with anti-CD63(LAMP3). The tetraspanin CD63(LAMP3) is a known marker for exosome biogenesis (36). Two independent ARPE clones (Fig. 1*A*, αB shRNA #1 and αB shRNA #2) were examined (Fig. 5*A*). There is a stark difference in the staining patterns between the controls (Fig. 5*A*, *Native ARPE* and cells transfected with a *Scrambled* sequence) and cells in which the αB expression is silenced (Fig. 5*A*, *αBshRNA #1* and *αBshRNA #2*). Both the clonal isolates showed similar patterns. CD63(LAMP3) staining is dispersed in the native ARPE cells and in cells transfected with the scrambled shRNA. In comparison, in cells where αB expression is inhibited, CD63(LAMP3) labeling is clumped in the perinuclear area (Fig. 5*A, αB shRNA #1* and *αB shRNA #2*, magnified cell, *open arrowheads,* and the corresponding surface plots in Fig. 5*B*) indicating that αB is required for the dispersed pattern seen in native wild-type cells and in cells transfected with scrambled shRNA sequence.

Importantly, although the distribution of the CD63(LAMP3)-fluorescence is different in the controls and in the αB-inhibited cells (Fig. 5*D*), total CD63(LAMP3) fluorescence in these cells remains largely unchanged (Fig. 5*C*, see also Fig. 8*D, immunoblot* for CD63(LAMP3)). Interestingly, αB and CD63(LAMP3) only show partial co-localization (in discrete dots that may represent MVBs or vesicles), suggesting that these two proteins are not directly interacting (15). These data (Fig. 5), coupled with the data from the sucrose density gradient analyses (Fig. 4), lead to the conclusion that in the absence of αB the CD63(LAMP3)-staining vesicles are made but are unable to traffic to or reach their presumed destination(s) within the cell.

Endolysosomal Compartment Is Enhanced in the Absence of αB—The data in Figs. 4 and 5 strongly indicate that in cells that do not make αB the synthesis of exosomes is not directly impacted but that their transport or the pathway that leads to their secretion may be blocked. Therefore, we reasoned that if the exosomes are made but are not secreted, they may progress to the endolysosomal compartment instead. To ascertain this, we first stained the cells with Lysotracker (Invitrogen) to assess

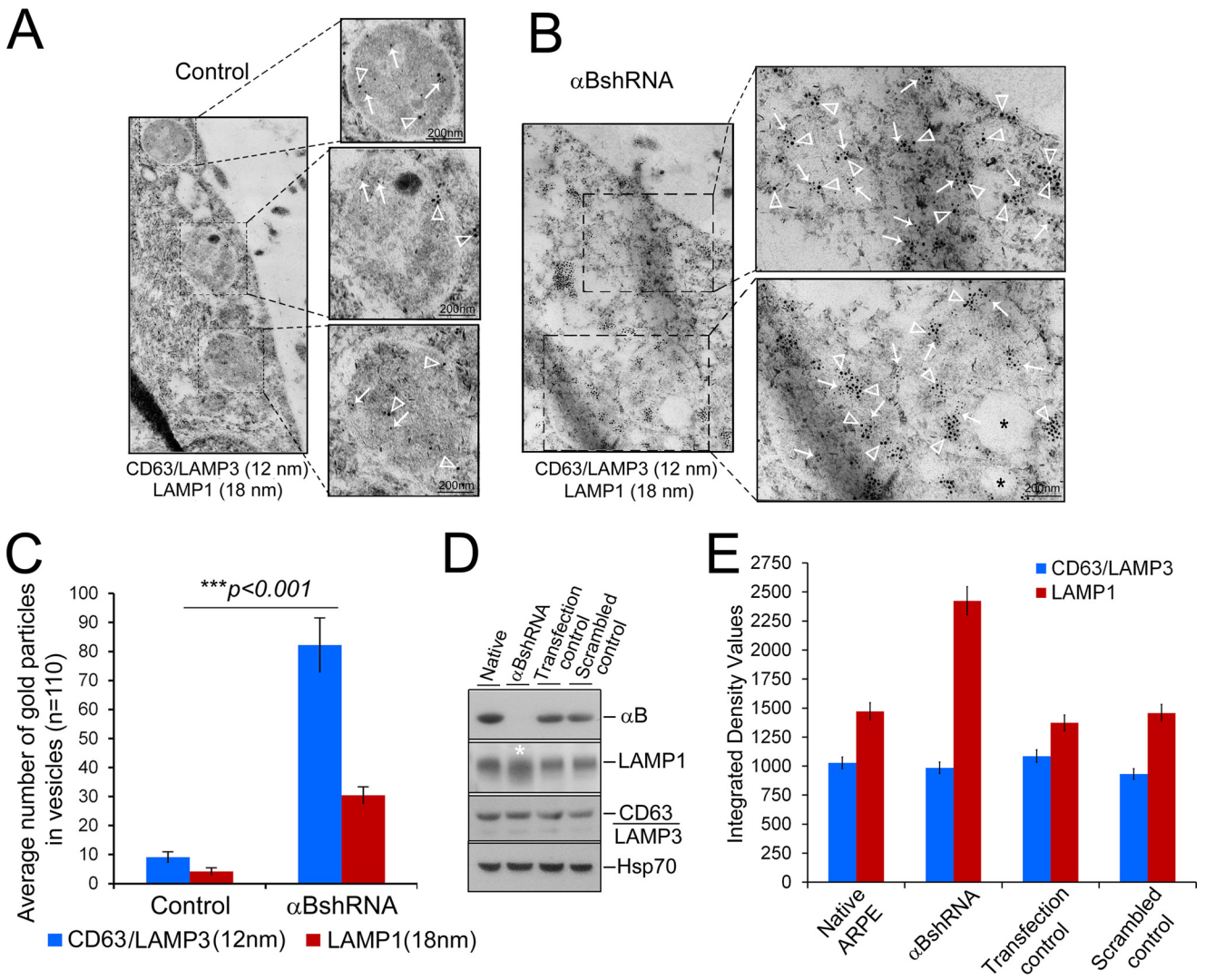

FIGURE 8. **Inhibition of the expression of αB leads to an enhancement of the endolysosomal compartment.** ARPE cell monolayers were gently scraped from the culture dish and processed for double immunogold labeling with anti-CD63 (LAMP3) (12-nm gold particles, endosomal marker) and anti-LAMP1 (18-nm gold particles, lysosomal marker). *A,* TEM of control ARPE cells show sparsely labeled CD63 (LAMP3) (*white arrows*) and LAMP1 (*white, open arrowheads*) in endolysosomes (*magnified images*). *B,* αB-silenced ARPE cells (*αBshRNA*) show clusters of 12-nm gold particles (CD63(LAMP 3) *white arrows*) and 18-nm gold particles (LAMP1, *white, open arrowheads*) within fused/enhanced endolysosomal vesicles (*magnified images on the right). C,* quantitation of the number of gold particles inside the vesicles in control and αB-silenced cells *(αBshRNA)* ($n = 110$, represent number of vesicles). *Asterisks* indicate statistically significant differences. ***, $p < 0.001$ (one-way analysis of variance followed by Tukey's post hoc test). *Scale bars,* 200 nm. *D,* immunoblot of whole cell extracts showing some enhancement of LAMP1 immune reaction (*white asterisks*) but no discernible change in CD63 (*LAMP3*) and HSP70 (run as an internal control). *E,* quantitation of the immunoblot shown in *D*. The control cells here are the transfected cells that did not show inhibition of αB expression (Fig. 1*A*, *Transfection control*).

the status of the lysosomes. We found that αB-silenced cells show excessive clumped staining (Fig. 6, *A* and *B*, compare *αB shRNA #1* and *αB shRNA #2* with the *Native* and *Scrambled* controls). Fig. 6*C* shows a tracing of the staining patterns clearly demonstrating aggregated lysosomal staining in cells that do not express αB (Fig. 6, *αB shRNA #1* and *αB shRNA # 2*).

TEM provides a better picture; it reveals that in cells where αB expression is inhibited, there seems to be an enhancement of the presence of fused vesicles and vacuoles (compare Fig. 7*A*, *control*, with Fig. 7*B*, *αBshRNA*). These cells show abnormally sized vesicles possibly as a result of fusions between MVBs/endosomes and lysosomes indicating the presence of an augmented endolysosomal compartment (compare Fig. 7, *A* with *B*).

The data shown in Fig. 7 are corroborated by double immunogold labeling with anti-CD63(LAMP3) (12-nm gold particles) and anti-LAMP1 (18-nm gold particles (Fig. 8, *A* and *B*). CD63 is also known as LAMP3. It is reported to be associated with late endosomes and lysosomal membranes (37). Based on the quantitation of the number of immunogold particles, CD63(LAMP3) shows a 6-fold increase, and LAMP1 shows a 10-fold increase between the control and αB-inhibited ARPE cells (Fig. 8*C*, *bar graph*). Immunoblotting for CD63 and LAMP1 in whole cell extracts shows an increase only in LAMP1 and no change in CD63 (Fig. 8, *C* and *D*), indicating that localized organelle-specific changes may not be detectable in a whole cell extract.

The data presented above in Figs. 5–9 suggest that in the absence of αB, the MVBs instead of progressing toward the plasma membrane progress toward the lysosome. It is possible that a block in the exosome secretion pushes the pathway toward the enhancement of the endosomal compartment through fusion of late endosomes with the lysosomes. To investigate whether this is the plausible scenario, we exam-

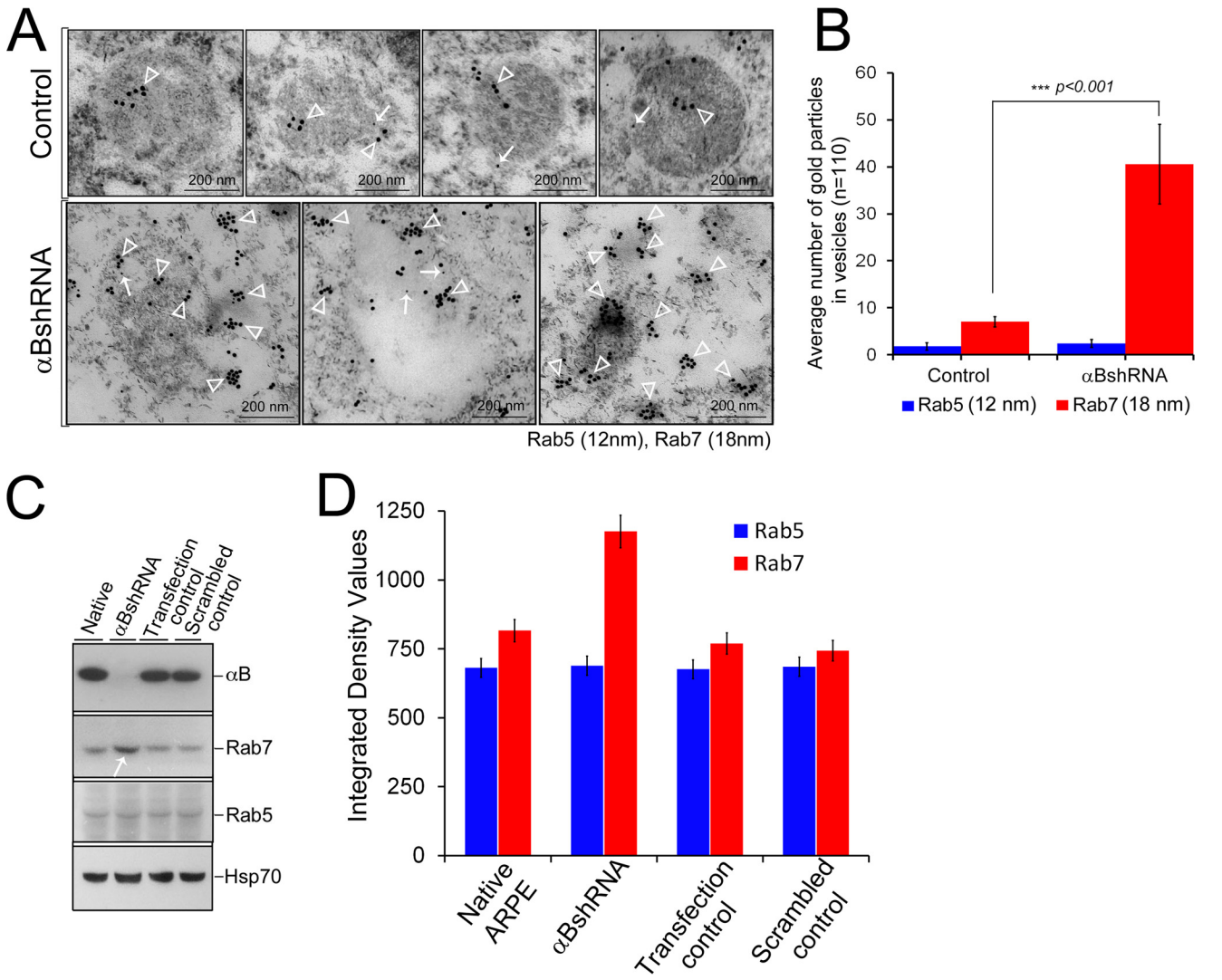

FIGURE 9. **Increased presence of Rab7 in αB-silenced ARPE cells.** ARPE cells were immunogold-labeled with anti-Rab5 (early endosome marker) and anti-Rab7 (late endosome marker). *A,* TEM of four endosomes from control ARPE cells (*top panel*) shows insignificant Rab5 labeling (12-nm gold particles) and moderately labeled Rab7 (18-nm gold particles). In contrast, there is enhanced immunolabeling of Rab7 (18-nm gold particles) in the endolysosomal compartment with no perceptible change in Rab5 (12-nm gold particles) in αB-silenced (*αBshRNA*) ARPE cells. Three micrographs of potentially fused vesicles (representing enhanced endolysosomal compartment) are shown. *B,* quantitation of immunogold labeling by ImageJ (analysis of particles) shows a 5-fold increase in Rab7 labeling but not in the Rab5. *C,* immunoblots of whole cell extracts for αB, Rab5, Rab7, and HSP70 in native, αB shRNA, transfection control, and scramble control ARPE cells. Note a noticeable increase in Rab7 in αB shRNA lane (*white arrow*) but no detectable change in Rab5 or HSP70 (run as an internal control). *D,* quantitation of the immunoblots shown in *C*. The data in *C* and *D* corroborate the TEM data in *A* and *B*.

ined the presence of two endosomal markers (Rab5 and Rab7) that are associated with the known dynamics of this pathway (38).

The two Rab GTPases, Rab5 and Rab7, are characteristically associated with the early endosome and the late endosome, respectively (39, 40). We examined their presence by immunogold labeling and TEM in the scrambled (control) and αB-silenced ARPE cells (Fig. 9). We do not see a significant labeling of Rab5 in either the control or in the αB-inhibited experimental cells, but we see a marked increase in the immunogold labeling of Rab7 in the fused vesicles characteristic of the ARPE cells where αB expression has been silenced (Fig. 9, *A* and *B*). The immunoblotting of whole cell extracts for Rab5 and Rab7 shows an increase in Rab7 but no change in Rab5 (Fig. 9, *C* and *D*). These data suggest that in the absence of αB, the late endosomes accumulate and therefore may contribute to the enhancement of the endolysosomal compartment in these cells (Fig. 10).

Discussion

In this investigation, we have demonstrated that the small heat shock protein αB is essential for the secretion of exosomes from the human ARPE19 cells. Although αB is secreted predominantly from the apical face of these cells (22), we find that inhibition of αB expression inhibits exosome secretion both from the apical as well as from the basal surfaces (Fig. 2). This suggests that αB may be involved in exosome biogenesis fairly early before any sorting of the exosomes to the basal or the apical surfaces takes place (41).

The data presented in Figs. 5 and 6 demonstrate that αB expression is essential for the normal dispersed pattern of CD63/LAMP3 and Lysotracker staining seen in the native

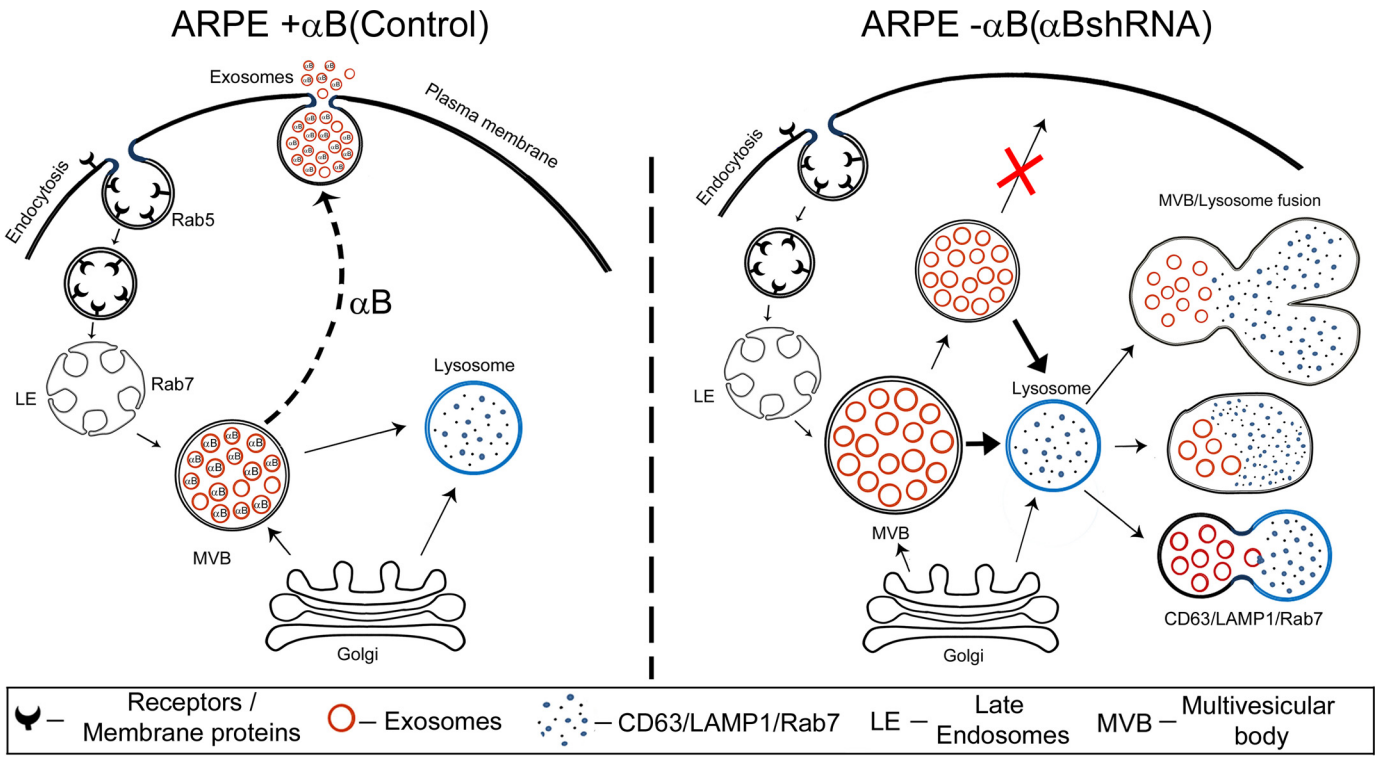

FIGURE 10. **Schematic representation of exosome biogenesis in presence and absence of αB expression in ARPE cells.** The *left schematic* shows facilitation of exosome secretion by αB in native ARPE cells (*αB on the dotted arrow* pointing to the plasma membrane). Note that we have shown αB inside the exosomes based on previously published work (22). It remains to be established whether all the exosomes contain αB; therefore, we have shown about 20% of the exosomes without αB. The *right schematic* shows enhancement of the endolysosomal compartment (fused vesicles) in the absence of αB in ARPE-αB shRNA cells. Note that this enhancement is consistent with the increase in the LAMP1 (Fig. 8) and Rab7 labeling in this compartment (Fig. 9).

ARPE cells and cells transfected with a scrambled sequence control (compare *Native ARPE* and *Scrambled* with αB *shRNA #1* and *#2*, Figs. 5 and 6). The impaired trafficking that is represented by aggregated staining patterns of CD63 (LAMP3) in the absence of αB (Fig. 5) leads to the conclusion that this small heat shock protein is involved in facilitating the secretion of exosomes.

The data presented here need to be understood in light of the knowledge that exosome biogenesis works normally in many cell types that do not express αB. Therefore, apparently αB represents one of the many cell type-specific proteins, which may be involved in exosome secretion. In other cells there must be other gene products that modulate/regulate exosome biogenesis (secretion) in a cell type-specific fashion. Whether there is a mechanistic relationship between secretion of a particular gene product in an exosome and its requirement outside of the cell is an interesting and an important question, which if understood may help with understanding the role of intercellular communication between cells in the sustenance of the final phenotype of a tissue and/or an organ. In the case of αB, its known propensity for binding to denatured polypeptides (10) without apparent specificity provides a logical reason for its protected presence within an exosome (22) that allows its distribution over longer distances without being hijacked.

How αB is involved in vesicle trafficking remains speculative at this time. It is possible that it regulates/facilitates traffic from the late endosome (or MVB) to the plasma membrane or alternatively to the lysosome. The increased labeling of CD63 (LAMP3) and LAMP1 (Fig. 8) suggests enhancement of the endolysosomal compartment, possibly because the passage of the MVB to the plasma membrane is impaired in the absence of αB. This is further supported by the accumulation of Rab7, a RabGTPase characteristic of the late endosomes (Fig. 9). These observations are in sync with the known enhancement of the endolysosomal compartment upon overexpression of Rab7 (42). It is unlikely that early endosome maturation is involved considering that we do not see any change in the Rab5 (a marker for early endosome maturation), either by immunoblotting or by TEM immunogold labeling in the control and the αB shRNA ARPE cells (Fig. 9). Overall, these data support the thesis that there is progression of the MVB toward the endolysosomal compartment in the absence of αB.

Although the exact sequence of events that incorporates αB into vesicles and then secretes them out of the RPE cell remains to be elucidated, based on the data presented above, it is possible to place this small heat shock protein at the branch point of exosome secretion and the endolysosomal compartment. In the native ARPE, which expresses αB constitutively, the MVB may progress away from the endolysosomal compartment, fuse with the plasma membrane, and release the exosomes. In the absence of αB, while the progression of the exosome-containing MVB toward the plasma membrane is blocked, the continued synthesis of exosomes may push the MVB to fuse with the lysosomes, leading to the enhancement of the endolysosomal compartment, evidenced here by enhanced immunogold labeling of CD63(LAMP3), LAMP1 (Fig. 8), and Rab7 (Fig. 9).

Based on the above discussion, we submit that αB is at the branch point of physiological decision making that facilitates

secretion of exosomes (Fig. 10). It is possible that various cell types have cell-specific regulators of this branch point thereby guiding what is sent for degradation inside the cell and what is sent outside of the cell.

Our interpretation of the data presented in this study may not be the only way αB is involved in vesicular trafficking and protein secretion. Although we find that the conventional protein secretion seems not to be directly impacted by the absence of αB (Fig. 3), suggesting an exosome-specific role for this protein, a mechanistic detail of how this protein interacts with the exosome secretory machinery remains to be delineated. It is possible that the reported anti-aggregation, chaperone-like property of αB (10) may become relevant to post-Golgi trafficking pathways (43, 44). It must also be recognized that there are multiple other unconventional ways of protein secretion (2, 45). The role of αB, if any, in any of these processes will require additional investigations.

The morphology of human retinal pigment epithelial (ARPE19) cells that do not make αB (αB shRNA) presents with prominent multivacuolated cytoplasm and enlarged vesicles predominantly near the perinuclear region and below the plasma membrane. We believe that the enlarged vesicles (endosomes and lysosomes) coalesce with vacuoles and generate large vesicle-vacuole hybrids, which contain densely stained material observable by electron microscopy (Fig. 7). The inhibition of the expression of αB and the increase in the number of vacuoles have been previously reported in the αB knock-out mice (46). Elucidation of the role of αB in the generation of vacuoles will entail a separate investigation that may enlighten the molecular pathogenesis, which leads to vacuolopathies associated with lysosomal dystrophies and neurodegenerations (31, 47).

Finally, it is important to recognize that RPE is an epithelium that is highly phagocytic, a role that sustains the turnover of the rod outer segments in the neuro-retina (5). The data presented in this study become an important starting point for dissecting the potential role of αB in the endosomal pathway and exosome secretion in the physiology and pathophysiology of this critical epithelium.

Author Contributions—R. K. G. conducted most of the experiments; A. B. transfected and screened the clones for αB expression; S. A. K. helped with TEM. S. P. B. conceived the project and wrote the manuscript with R. K. G.

Acknowledgments—We thank Ishanee Dighe and Ayushi Neogi for help with immunoblotting. We thank Dennis Mock for help with presentation of the data and useful suggestions and Dr. Joseph Horwitz for input and discussions. We also thank Marianne Cilluffo for help with TEM.

References

1. Hanson, P. I., and Cashikar, A. (2012) Multivesicular body morphogenesis. *Annu. Rev. Cell Dev. Biol.* **28,** 337–362
2. Manjithaya, R., and Subramani, S. (2011) Autophagy: a broad role in unconventional protein secretion? *Trends Cell Biol.* **21,** 67–73
3. Simons, M., and Raposo, G. (2009) Exosomes–vesicular carriers for intercellular communication. *Curr. Opin. Cell Biol.* **21,** 575–581
4. Zhang, M., and Schekman, R. (2013) Cell biology. Unconventional secretion, unconventional solutions. *Science* **340,** 559–561
5. Bok, D. (1985) Retinal photoreceptor-pigment epithelium interactions. Friedenwald lecture. *Invest. Ophthalmol. Vis. Sci.* **26,** 1659–1694
6. Fuhrmann, S., Zou, C., and Levine, E. M. (2014) Retinal pigment epithelium development, plasticity, and tissue homeostasis. *Exp. Eye Res.* **123,** 141–150
7. De, S., Rabin, D. M., Salero, E., Lederman, P. L., Temple, S., and Stern, J. H. (2007) Human retinal pigment epithelium cell changes and expression of αB-crystallin: a biomarker for retinal pigment epithelium cell change in age-related macular degeneration. *Arch. Ophthalmol.* **125,** 641–645
8. Bhat, S. P. (2003) Crystallins, genes and cataract. *Prog. Drug Res.* **60,** 205–262
9. Andley, U. P. (2007) Crystallins in the eye: function and pathology. *Prog. Retin. Eye Res.* **26,** 78–98
10. Horwitz, J. (2000) The function of α-crystallin in vision. *Semin. Cell Dev. Biol.* **11,** 53–60
11. Kibbelaar, M. A., and Bloemendal, H. (1979) Fractionation of the water-soluble proteins from calf lens. *Exp. Eye Res.* **29,** 679–688
12. Cobb, B. A., and Petrash, J. M. (2000) Characterization of α-crystallin-plasma membrane binding. *J. Biol. Chem.* **275,** 6664–6672
13. Gangalum, R. K., Schibler, M. J., and Bhat, S. P. (2004) Small heat shock protein αB-crystallin is part of cell cycle-dependent Golgi reorganization. *J. Biol. Chem.* **279,** 43374–43377
14. Gangalum, R. K., and Bhat, S. P. (2009) αB-crystallin: a Golgi-associated membrane protein in the developing ocular lens. *Invest. Ophthalmol. Vis. Sci.* **50,** 3283–3290
15. Bhat, S. P., and Gangalum, R. K. (2011) Secretion of αB-crystallin via exosomes: new clues to the function of human retinal pigment epithelium. *Commun. Integr. Biol.* **4,** 739–741
16. Bhat, S. P., and Nagineni, C. N. (1989) αB subunit of lens-specific protein α-crystallin is present in other ocular and non-ocular tissues. *Biochem. Biophys. Res. Commun.* **158,** 319–325
17. D'Antonio, M., Michalovich, D., Paterson, M., Droggiti, A., Woodhoo, A., Mirsky, R., and Jessen, K. R. (2006) Gene profiling and bioinformatic analysis of Schwann cell embryonic development and myelination. *Glia* **53,** 501–515
18. Bsibsi, M., Peferoen, L. A., Holtman, I. R., Nacken, P. J., Gerritsen, W. H., Witte, M. E., van Horssen, J., Eggen, B. J., van der Valk, P., Amor, S., and van Noort, J. M. (2014) Demyelination during multiple sclerosis is associated with combined activation of microglia/macrophages by IFN-γ and αB-crystallin. *Acta Neuropathol.* **128,** 215–229
19. Nagineni, C. N., and Bhat, S. P. (1989) αB-crystallin is expressed in kidney epithelial cell lines and not in fibroblasts. *FEBS Lett.* **249,** 89–94
20. Jing, Z., Gangalum, R. K., Lee, J. Z., Mock, D., and Bhat, S. P. (2013) Cell-type-dependent access of HSF1 and HSF4 to αB-crystallin promoter during heat shock. *Cell Stress Chaperones* **18,** 377–387
21. Alge, C. S., Priglinger, S. G., Neubauer, A. S., Kampik, A., Zillig, M., Bloemendal, H., and Welge-Lussen, U. (2002) Retinal pigment epithelium is protected against apoptosis by αB-crystallin. *Invest. Ophthalmol. Vis. Sci.* **43,** 3575–3582
22. Gangalum, R. K., Atanasov, I. C., Zhou, Z. H., and Bhat, S. P. (2011) αB-crystallin is found in detergent-resistant membrane microdomains and is secreted via exosomes from human retinal pigment epithelial cells. *J. Biol. Chem.* **286,** 3261–3269
23. Villarroya-Beltri, C., Baixauli, F., Gutiérrez-Vázquez, C., Sánchez-Madrid, F., and Mittelbrunn, M. (2014) Sorting it out: regulation of exosome loading. *Semin. Cancer Biol.* **28,** 3–13
24. Brinton, L. T., Sloane, H. S., Kester, M., and Kelly, K. A. (2015) Formation and role of exosomes in cancer. *Cell. Mol. Life Sci.* **72,** 659–671
25. Baietti, M. F., Zhang, Z., Mortier, E., Melchior, A., Degeest, G., Geeraerts, A., Ivarsson, Y., Depoortere, F., Coomans, C., Vermeiren, E., Zimmermann, P., and David, G. (2012) Syndecan-syntenin-ALIX regulates the biogenesis of exosomes. *Nat. Cell Biol.* **14,** 677–685
26. Duran, J. M., Campelo, F., van Galen, J., Sachsenheimer, T., Sot, J., Egorov, M. V., Rentero, C., Enrich, C., Polishchuk, R. S., Goñi, F. M., Brügger, B., Wieland, F., and Malhotra, V. (2012) Sphingomyelin organization is required for vesicle biogenesis at the Golgi complex. *EMBO J.* **31,** 4535–4546

27. Hurley, J. H., and Odorizzi, G. (2012) Get on the exosome bus with ALIX. *Nat. Cell Biol.* **14,** 654–655
28. Yang, J. M., and Gould, S. J. (2013) The cis-acting signals that target proteins to exosomes and microvesicles. *Biochem. Soc. Trans.* **41,** 277–282
29. Zhu, H., Guariglia, S., Yu, R. Y., Li, W., Brancho, D., Peinado, H., Lyden, D., Salzer, J., Bennett, C., and Chow, C. W. (2013) Mutation of SIMPLE in charcot-marie-tooth 1C alters production of exosomes. *Mol. Biol. Cell* **24,** 1619–1637
30. Savina, A., Furlán, M., Vidal, M., and Colombo, M. I. (2003) Exosome release is regulated by a calcium-dependent mechanism in K562 cells. *J. Biol. Chem.* **278,** 20083–20090
31. Tagliaferro, P., Kareva, T., Oo, T. F., Yarygina, O., Kholodilov, N., and Burke, R. E. (2015) An early axonopathy in a hLRRK2(R1441G) transgenic model of Parkinson disease. *Neurobiol. Dis.* **82,** 359–371
32. Willem, J., ter Beest, M., Scherphof, G., and Hoekstra, D. (1990) A non-exchangeable fluorescent phospholipid analog as a membrane traffic marker of the endocytic pathway. *Eur. J. Cell Biol.* **53,** 173–184
33. Gangalum, R. K., Horwitz, J., Kohan, S. A., and Bhat, S. P. (2012) αA-crystallin and αB-crystallin reside in separate subcellular compartments in the developing ocular lens. *J. Biol. Chem.* **287,** 42407–42416
34. Persson, S., and Havton, L. A. (2009) Retrogradely transported fluorogold accumulates in lysosomes of neurons and is detectable ultrastructurally using post-embedding immuno-gold methods. *J. Neurosci. Methods* **184,** 42–47
35. An, E., Gordish-Dressman, H., and Hathout, Y. (2008) Effect of TNF-α on human ARPE-19-secreted proteins. *Mol. Vis.* **14,** 2292–2303
36. Mathivanan, S., and Simpson, R. J. (2009) ExoCarta: A compendium of exosomal proteins and RNA. *Proteomics* **9,** 4997–5000
37. Kobayashi, T., Vischer, U. M., Rosnoblet, C., Lebrand, C., Lindsay, M., Parton, R. G., Kruithof, E. K., and Gruenberg, J. (2000) The tetraspanin CD63/lamp3 cycles between endocytic and secretory compartments in human endothelial cells. *Mol. Biol. Cell* **11,** 1829–1843
38. Segev, N. (2011) Coordination of intracellular transport steps by GTPases. *Semin. Cell Dev. Biol.* **22,** 33–38
39. Feng, Y., Press, B., and Wandinger-Ness, A. (1995) Rab 7: an important regulator of late endocytic membrane traffic. *J. Cell Biol.* **131,** 1435–1452
40. Zerial, M., and McBride, H. (2001) Rab proteins as membrane organizers. *Nat. Rev. Mol. Cell Biol.* **2,** 107–117
41. Lobert, V. H., and Stenmark, H. (2011) Cell polarity and migration: emerging role for the endosomal sorting machinery. *Physiology* **26,** 171–180
42. Bucci, C., Thomsen, P., Nicoziani, P., McCarthy, J., and van Deurs, B. (2000) Rab7: a key to lysosome biogenesis. *Mol. Biol. Cell* **11,** 467–480
43. Keller, P., and Simons, K. (1997) Post-Golgi biosynthetic trafficking. *J. Cell Sci.* **110,** 3001–3009
44. Robinson, D. G., and Pimpl, P. (2014) Clathrin and post-Golgi trafficking: a very complicated issue. *Trends Plant Sci.* **19,** 134–139
45. Nickel, W. (2005) Unconventional secretory routes: direct protein export across the plasma membrane of mammalian cells. *Traffic* **6,** 607–614
46. Brady, J. P., Garland, D. L., Green, D. E., Tamm, E. R., Giblin, F. J., and Wawrousek, E. F. (2001) αB-crystallin in lens development and muscle integrity: a gene knockout approach. *Invest. Ophthalmol. Vis. Sci.* **42,** 2924–2934
47. Perrett, R. M., Alexopoulou, Z., and Tofaris, G. K. (2015) The endosomal pathway in Parkinson's disease. *Mol. Cell. Neurosci.* **66,** 21–28